Hindawi
Advances in Condensed Matter Physics
Volume 2019, Article ID 4949365, 8 pages
https://doi.org/10.1155/2019/4949365

Research Article

Influence of Crystallization Time on Energy-Storage Density and Efficiency of Lead-Free $Bi_{0.5}(Na_{0.8}K_{0.2})_{0.5}TiO_3$ Thin Films

Ngo Duc Quan,[1,2] **Tran Quoc Toan**,[3,4] **and Vu Ngoc Hung**[2]

[1] *School of Engineering Physics, Ha Noi University of Science and Technology, 1 Dai Co Viet Road, Hanoi 100000, Vietnam*
[2] *International Training Institute for Materials Science, Hanoi University of Science and Technology, 1 Dai Co Viet Road, Hanoi 100000, Vietnam*
[3] *Graduate University of Science and Technology, Vietnam Academy of Science and Technology, 18 Hoang Quoc Viet Road, Hanoi 100000, Vietnam*
[4] *Institute of Natural Products Chemistry, Vietnam Academy of Science and Technology, 18 Hoang Quoc Viet Road, Hanoi 100000, Vietnam*

Correspondence should be addressed to Ngo Duc Quan; quan.ngoduc@hust.edu.vn

Received 7 September 2018; Revised 4 November 2018; Accepted 16 December 2018; Published 1 January 2019

Guest Editor: Hong Fang

Lead-free $Bi_{0.5}(Na_{0.80}K_{0.20})_{0.5}TiO_3$ (BNKT) ferroelectric films were synthesized on Pt/Ti/SiO_2/Si substrates via chemical solution deposition. The influence of crystallization time on the microstructures and ferroelectric and energy-storage properties of the films was investigated in detail. The XRD analysis showed that the BNKT films have well crystallized corresponding to the single-phase perovskite structure at 700°C. Ferroelectric and energy-storage properties of the films were significantly enhanced by increasing crystallization time. With crystallization time of 60 min, the remnant polarization (P_r), maximum polarization (P_m), and P_m-P_r values reached the highest values of 7.9 μC/cm^2, 28.9 μC/cm^2, and 21.0 μC/cm^2, respectively, under the electric field of 400 kV/cm. Thanks to the strong enhancement in P_m and the large P_{ma}-P_r value, the highest recoverable energy-storage density (J_{reco}) gets the value of 2.9 J/cm^3. The obtained results indicate that the BNKT films have application potentials in advanced capacitors.

1. Introduction

Recently, people have faced big global challenges such as the air pollution, climate change, and the energy scarcity. For the sustainable development, the traditional fossil fuel energy resources should be replaced by new energy generation technologies, such as wind and solar and thermal energy with cleaner renewable sources. Hence, the development of the high energy-storage materials and devices has been paid increasing attention. The dielectric capacitors owning numerous good properties such as ultrafast charge-discharge rate, high energy-storage density (J_{reco}), good temperature stability, and low cost have been widely studied in the past decades. They have been used in a lot of modern electrical equipment, such as high power microwaves and electromagnetic armor. [1–5]. Because of the integrating and miniaturizing tendency of electronic devices, an ideal capacitor needs to possess high energy-storage density, rapid discharge, and high energy-storage efficiency (η) [1, 6, 7]. Theoretically, the dielectric materials having the small remnant polarization (P_r), high saturated polarization (P_m), and high breakdown strength (BDS) are the most potential candidates [1]. By far, majority of studies on film capacitors have been just focused on lead-based materials (PZT) [5, 8–12]. However, owing to containing high Pb content, PZT-based materials are not environmentally friendly and likely harm the human health. Hence, the developments of lead-free materials with high J_{reco} and η are an urgent demand for the applications of pulsed power capacitors. Currently, lead-free ceramics, such as $(K_{0.5}Na_{0.5})NbO_3$ (KNN)-based [13], $BaTiO_3$ (BT)-based [14], SrTiO3 (ST)-based [3], and $(Bi_{0.5}Na_{0.5})TiO_3$ (BNT)-based [15], have attracted much attention because of their good energy-storage properties. Among them, lead-free $(Na_{0.5}Bi_{0.5})TiO_3$ (NBT) ferroelectric materials have been

extensively investigated for mainly the past 10 years [16]. Smolenski and his coworkers [17] revealed NBT as typical perovskite-type ferroelectrics in 1961. When modified by other ABO_3 phases, the critical temperature at which the AF-AFE phase transition occurs could be reduced with an increase of ferroelectric properties. For example, NBT–xBT lead-free thick films [18] were studied on the temperature-dependence of the J_{reco} and leakage current performance. Authors attained the enhancement of the BDS and the $P_m - P_r$ value for NBT–0.06BT, resulting in the improvements of energy-storage properties (the maximum J_{reco} and η of 2.3 J/cm^3 and 45%, respectively at under 550 kV/cm). Xu and his coworkers [19] obtained the solid solubility of BNTBT with NBN and optimized energy-storage properties with J_{reco} = 1.36 J/cm^3 and η = 73.9 % at NBN content of 0.02. For the same system, Lu et al. [20], thanks to the La and Zr codoping, enhanced the energy-storage capacity of the BNTBT (the maximum J_{reco} was 1.21 J/cm^3 at 100 kV/cm). In the report [20], the energy-storage density of BNBT–xKN ceramics was explored with the rise of KN addition. Authors indicated that the energy-storage density is increased radically and reached the maximum value of 0.89 J/cm^3 at 100 kV/cm for BNBT–0.06KN. $(1 - x)$BNTBT-xNN ceramics [15], prepared via the conventional solid state reaction method, exhibit more slim P–E loops with increasing the NN amount. Therefore, the J_{reco} was enhanced significantly and reached the highest value of 0.71 J/cm^3 for x = 0.10 at 7 kV/mm. Being similar AFE ceramic, $(1–x)(Na_{0.5}Bi_{0.5})TiO_3–xSrTiO_3$ (NBT-ST) system was reported by Cao et al. [21]. The 0.7NBT-0.3ST exhibited excellent temperature stability in its energy-storage density from the room temperature to 120°C with the maximum J_{reco} value of 0.65 J/cm^3 obtained at 65 kV/cm. Via a solid–solid state route, 0.475BNT–0.525BCTZ–x wt% MgO ceramics [22] were prepared and we investigated their phase structure, microstructure and dielectric and energy-storage properties with the focus on optimizing properties for capacitor applications. Thanks to significant enhancement of the dielectric breakdown strength in these ceramics with the addition of MgO, their discharge energy density was strongly improved. With a high dielectric breakdown strength of 15.67 kV/mm, the sample with x = 5 showed the highest maximum J_{reco} of 1.04 J/cm^3. Comparing to bulk ceramics, the ferroelectric films having the higher BDS could release the drawbacks of bulk ceramics and be suitable for the high energy-storage applications. NBT films [23] synthesized on LNO/Si (100) substrates by using a sol-gel technique show the excellent energy-storage properties with the J_{reco} of 12.4 J/cm^3 and η of 43% at 1200 kV/cm. Zhang et al. [24] markedly enhanced the energy-storage properties of 0.7NBT-0.3ST relaxor films by the Mn^{2+} substitution for Ti^{4+}. With appropriate Mn doping (1mol. %), the highest J_{reco} value of 27 J/cm^3 was gained thanks to the high BDS value of 1894 kV/cm.

The above studies indicated that the energy-storage density was significantly improved by enlarging the difference value between P_m and P_r and/or increasing the value of breakdown strength (BDS). Enhancement of J_{reco} value in lead-free thin films has gained the progress, but their performances were still far inferior to those of lead-based materials. The processing conditions of NBT-based films (such as the annealing temperature and crystallization time), which contribute closely to the quality and cost of products, were rarely studied. In the present study, we fabricated lead-free $Bi_{0.5}(Na_{0.8}K_{0.2})_{0.5}TiO_3$ (abbreviated as BNKT) films via a sol-gel method on Pt/Ti/SiO_2/Si substrates and investigated the energy-storage properties of BNKT films annealed at 700°C as a function of annealing time (10 min, 20 min, 40 min, and 60 min). We found that ferroelectric and energy-storage properties were enhanced when the annealing time was increased.

2. Materials and Methods

The $Bi_{0.5}(Na_{0.80},K_{0.20})_{0.5}TiO_3$ (BNKT) thin films were formed on Pt/Ti/SiO_2/Si substrates by a sol-gel technique. Here, the BNKT precursor solutions are derived from sodium nitrate ($NaNO_3$, ≥99%, Sigma-Aldrich), potassium nitrate (KNO_3, ≥99%, Sigma-Aldrich), bismuth nitrate ($Bi(NO_3)_3{\cdot}5H_2O$, ≥98%, Sigma-Aldrich), and titanium isopropoxide (Ti[i-OPr]$_4$, 99%, Sigma-Aldrich). Acetic acid and 2-methoxyethanol were chosen as cosolvent, and acetylacetones were chosen as ligands. During the process, titanium isopropoxide was at first dissolved in acetylacetone to prevent its hydrolysis. In order to compensate the possible Na and K loss during high temperature annealing, we added their excess amounts of 30% and 20%, respectively. The mixture was stirred at 70°C for 6 hours constantly to form the final solution until a 0.4 M transparent and stable yellow precursor solution was obtained. Each layer of the BNKT films was formed by spin coating 0.4 M precursor on substrates at 4000 rpm for 30 s, followed by pyrolysis at 400°C for 10 min. The process was repeated until the BNKT thin films with the required coating layers were obtained. Finally, BNKT thin films were annealed at 700°C in different periods (10 min, 20 min, 40 min, and 60 min) to obtain the ferroelectric phase. For the convenience, these films were named as T10, T20, T40, and T60, respectively.

Characteristics of the films as the cross-sectional and surface morphologies were detected by a field emission *scanning electron microscope* (FE-SEM, Hitachi S4800) and atomic force microscopy (AFM, Bruker Dimension ICON). The crystal structures of BNKT thin films were characterized by a Bruker D5005 diffractometer using Cu-Kα radiation (λ = 1.5406 Å). P–E hysteresis loops were measured under the applied voltages ranging from −25 V to 25 V, frequency of 1000 Hz by using a TF Analyzer 2000 ferroelectric tester (aixACCT Systems GmbH, Germany).

3. Results and Discussion

The BNKT films, after a synthesis, were investigated to check the surface morphology and roughness by using the SEM and AFM techniques. The two-dimensional (2D) and three-dimensional (3D) AFM images for the BNKT films scanned over a surface area of 40 μm × 40 μm were described in detail in Figures 1(a)–1(d). The AFM images revealed the densely packed, crack-free, uniform surfaces with the grains possessing columnar shape. The roots mean square

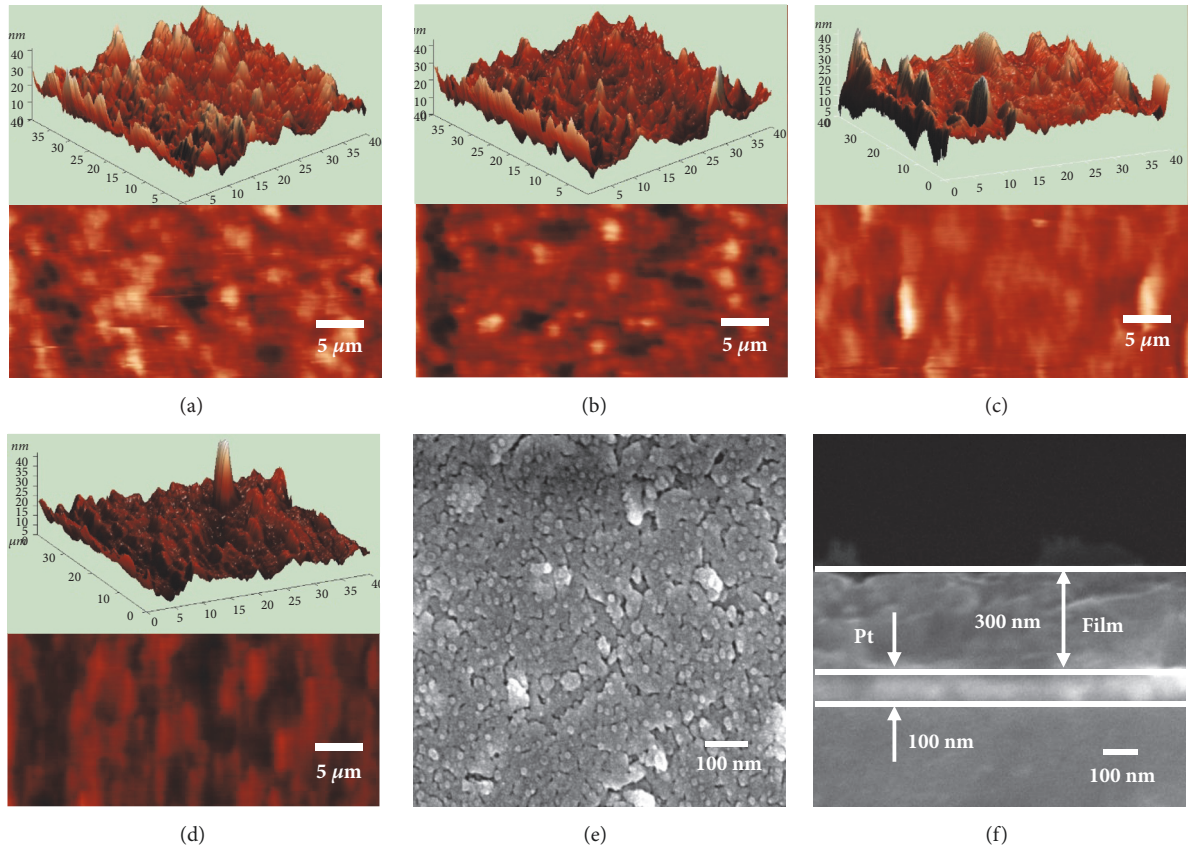

FIGURE 1: Two-dimensional (2D) and three-dimensional (3D) AFM images of BNKT films: (a) T10, (b) T20, (c) T40, (d) T60, (e) FE-SEM micrographs of sample T60, and (f) cross-sectional SEM image of sample T60.

surface roughness (R_{rms}) was calculated and shown in the Table 1. R_{rms} possesses the values of 5.5, 4.8, 4.6, and 3.8 nm corresponding to the BNKT films: T10, T20, T40, and T60. The low R_{rms} values of the film surfaces evidence a smooth morphology. The decrease of R_{rms} with annealing time is mainly due to the growth of BNKT crystallite with smaller grain boundaries merged into larger ones. The surface morphology of the BNKT thin films, therefore, becomes denser with an increase of the annealing time. This AFM result was also consistent with the analysis exposed by the XRD characterization and FE-SEM micrographs. In Figure 1(e), we demonstrated the FE-SEM micrograph of sample T60 annealed in 60 min. This thin film was shown to exhibit a dense and smooth surface consisting of tetragonal grain size particles without any traces of cracks detected. Figure 1(f) displayed the cross-sectional FE-SEM image of the T60 film. Based on this analysis, we can determine thicknesses of films, around 300 nm.

The BNKT thin film structure was measured with a θ-2θ mode in steps of 0.02°. Figure 2(a) displays the XRD patterns of the BNKT films associated with the conditions of annealed at 700°C for different durations. The angular peak positions of the XRD signals are observed at around 2θ: 31.2°, 39.8°, 47.3°, and 58.0° corresponding to the BNKT bulk [24]. With the surpassed intensity, the (111) orientation located at $2\theta \sim 39.8°$ is the mixture of orientations, deriving from the Pt coated substrate. All other peaks belong to a single-phase perovskite structure with no other impurity phases detected, which agrees with our recent report [25] on influence of crystallization temperature on multiferroic behaviour of BNKT films. This observation also matches our previous works [26, 27] where they indicated that BNKT thin films possess simultaneously the rhombohedral and tetragonal symmetries. Among the typical orientations of the perovskite structure, the (110)/(200) peaks possess high intensity and therefore are the preferred orientations of the films. These intensity peaks were demonstrated in Figures 2(b) and 2(c) with the 2θ ranges: (b) 30.0°–34.0° and (c) 46.0°–48.5°. Analysed result shows that the (200) peak intensity of the BNKT films obviously tends to rise when annealing time increases from 10 min to 60 min. The full width at half maximum (FWHM) evaluated from the XRD patterns declines with increasing annealing time. This proved that the grain size enlarged as the annealing time was increased. To specify, we evaluated the grain size of films by using Scherrer equation [28]:

$$D = \frac{K \cdot \lambda}{\beta \cdot \cos\theta} \quad (1)$$

where D, K, λ, β, and θ are grain size, constant of crystallite shape (normally taken as 0.9), wave length, FWHM, and

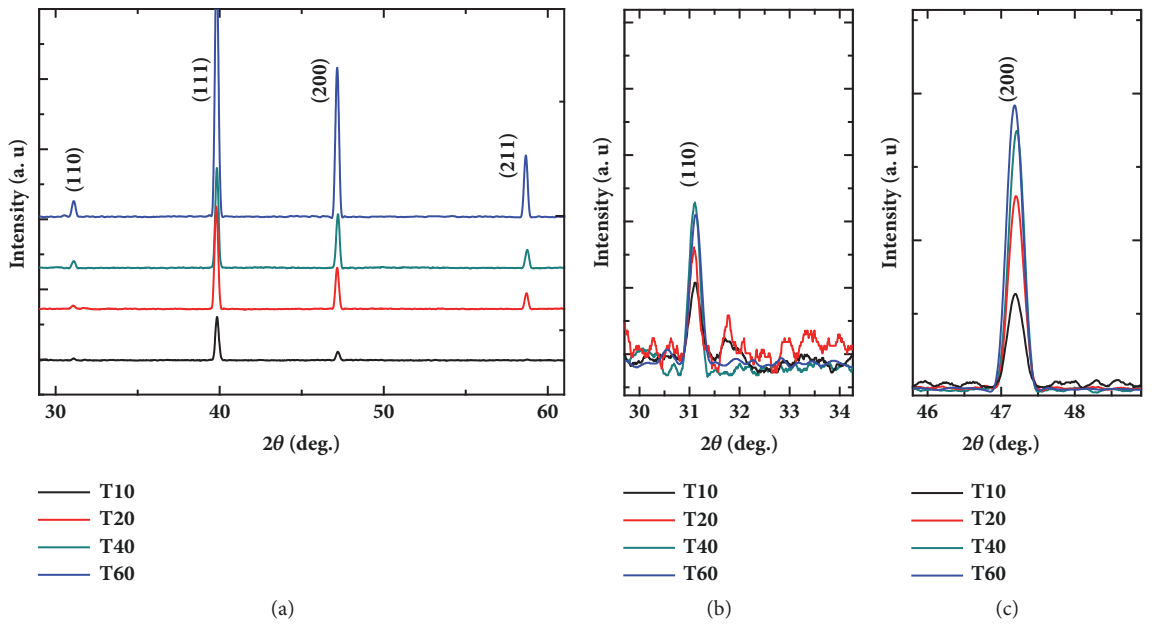

FIGURE 2: X-ray diffraction patterns of BNKT films in the 2θ ranges of (a) 28.0°–62.0°, (b) 30.0°–34.0°, and (c) 46.0°–48.5°.

TABLE 1: The grain size and roots mean square roughness as a function of the annealing time.

Annealing time (min)	10	20	40	60
Grain size, D (nm)	44.9	47.2	49.1	49.7
Roots mean square roughness, R_{rms} (nm)	5.5	4.8	4.6	3.8

Bragg angle, respectively. The grain size was calculated and illustrated as a function of the annealing time in the Table 1. D value increased significantly from 44.9 nm for the film T10 to 49.7 nm for the film T60.

Furthermore, the XRD analysis about the film structure was confirmed by Raman technique with higher sensitivity. Figures 3(a)–3(d) show the Raman spectra of BNKT films as a function of crystallization time in the wavenumber ranges of 100–1000 cm^{-1} at room temperature. Lorentzian fitting technique was employed to expose the typical peaks of a perovskite structure. The Raman result is consistent with previous work on BNKTS ceramics [29], where it reported that A_1(TO1) mode at ~138 cm^{-1} is assigned to the A-site vibrations. For the film, this mode corresponds to the wavenumber of 118 cm^{-1}. We also observed the B_1(TO1) mode at 281 cm^{-1}, assigned to O-Ti-O bending motion [30]. Especially, Chen and his coworkers [29, 31] revealed the modes at higher wavenumbers, such as the A_1(TO3) at 525 cm^{-1} and E(LO) at 615 cm^{-1} characterizing for vibrations of TiO_6 oxygen octahedral. For our study, these modes are located at 514 cm^{-1} and 590 cm^{-1}, respectively. The wavenumber differences may be caused by the residual stress formed by film/substrate interface. Similar behaviour is also observed in our recent works [25, 32].

Ferroelectric properties of the BNKT films were examined by using a TF Analyzer 2000 ferroelectric tester at 1 kHz at room temperature. Figures 4(a)–4(d) illustrate the P–E loops for the BNKT films with different crystallization times. In Figure 4, the P_m, P_r, and P_m - P_r values of the films were evaluated and analysed. An obvious enhancement of the ferroelectricity can be observed as the annealing time increases. When being annealed in 10 min, BNKT films show a relatively poor ferroelectricity with small P_m, P_r, and P_m - P_r values of around 18.9 $\mu C/cm^2$, 4.1 $\mu C/cm^2$, and 14.8 $\mu C/cm^2$, respectively. These values continuously increase as the annealing time is raised. Especially, at annealing time of 60 min, the P_m, P_r, and P_m - P_r reach their highest values of around 28.9 $\mu C/cm^2$, 7.9 $\mu C/cm^2$, and 21.0 $\mu C/cm^2$, respectively. The increase in the ferroelectric properties matches up the grain size change and phase transition observed from the XRD analysis. With the annealing time ≥ 60 min, the intermediate pyrochlore phase completely transformed into the perovskite phase, and therefore the polarization in the film is improved. Furthermore, BNKT films revealed a great difference between the maximum polarization (P_m) and remnant polarization (P_r). Ahn and his coworkers [33] also reported similar behaviour, which resulted from the strong transform in the domain configuration between the states: (i) applying the electric field and (ii) removing the electric field. Because of the tensile stress at the film/substrate interface, domains may easily switch their original states as the electric field decreases to zero, leading to the small net polarization. By contrast, at a high electric field, BNKT films reach the spontaneous polarization of the bulk materials thanks to the

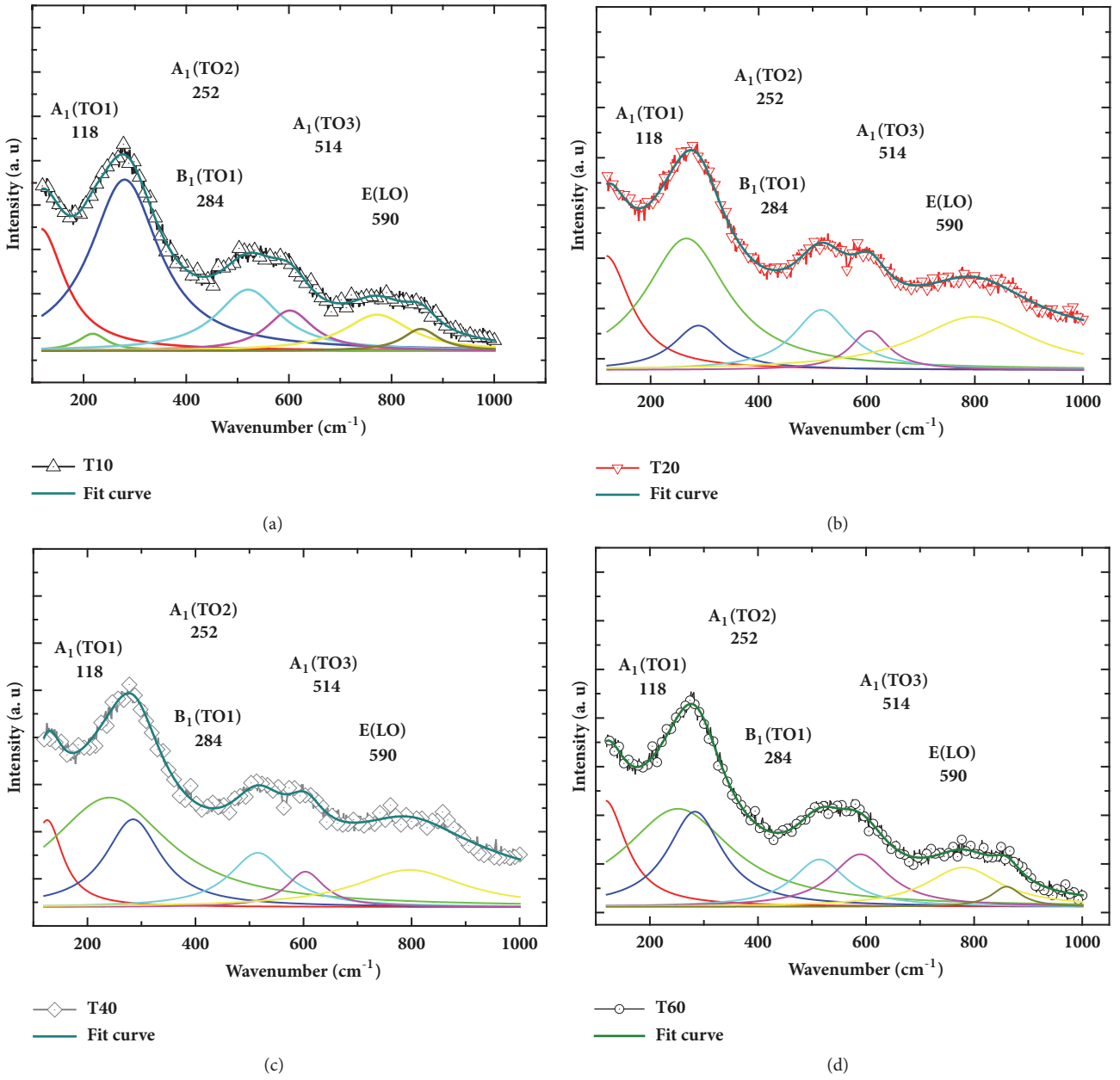

FIGURE 3: Raman spectra of BNKT films with different annealing times in the wavenumber ranges of 100–1000 cm^{-1}.

domain reorientation induced by the applied electric field. A high ($P_m - P_r$) value is a useful parameter for the energy-storage devices.

The energy-storage properties of the BNKT films were calculated based on the schematic diagram in Figure 5(a). J_{reco} is the recoverable electrical-energy density stored in the dielectric films and calculated from *P-E* hysteresis loops by the following expression [34]:

$$J_{reco} = \int_{P_r}^{P_m} EdP \tag{2}$$

where E refers to the applied electric field and P_m and P_r are the maximum and remnant polarization values, respectively. J_{loss} is the energy corresponding to the inherent hysteresis in the material. It is defined as numerical integration of closed area of the hysteresis loops (Figure 5(a)). The total energy (J_{total}) needs to charge a ferroelectric capacitor which is the sum of dielectric losses (J_{loss}) and recoverable (J_{reco}) energy. Thus, J_{loss} and J_{total} can be represented as

$$J_{loss} = \int_{0}^{P_r} EdP$$
$$\text{and } J_{total} = J_{reco} + J_{loss} \tag{3}$$

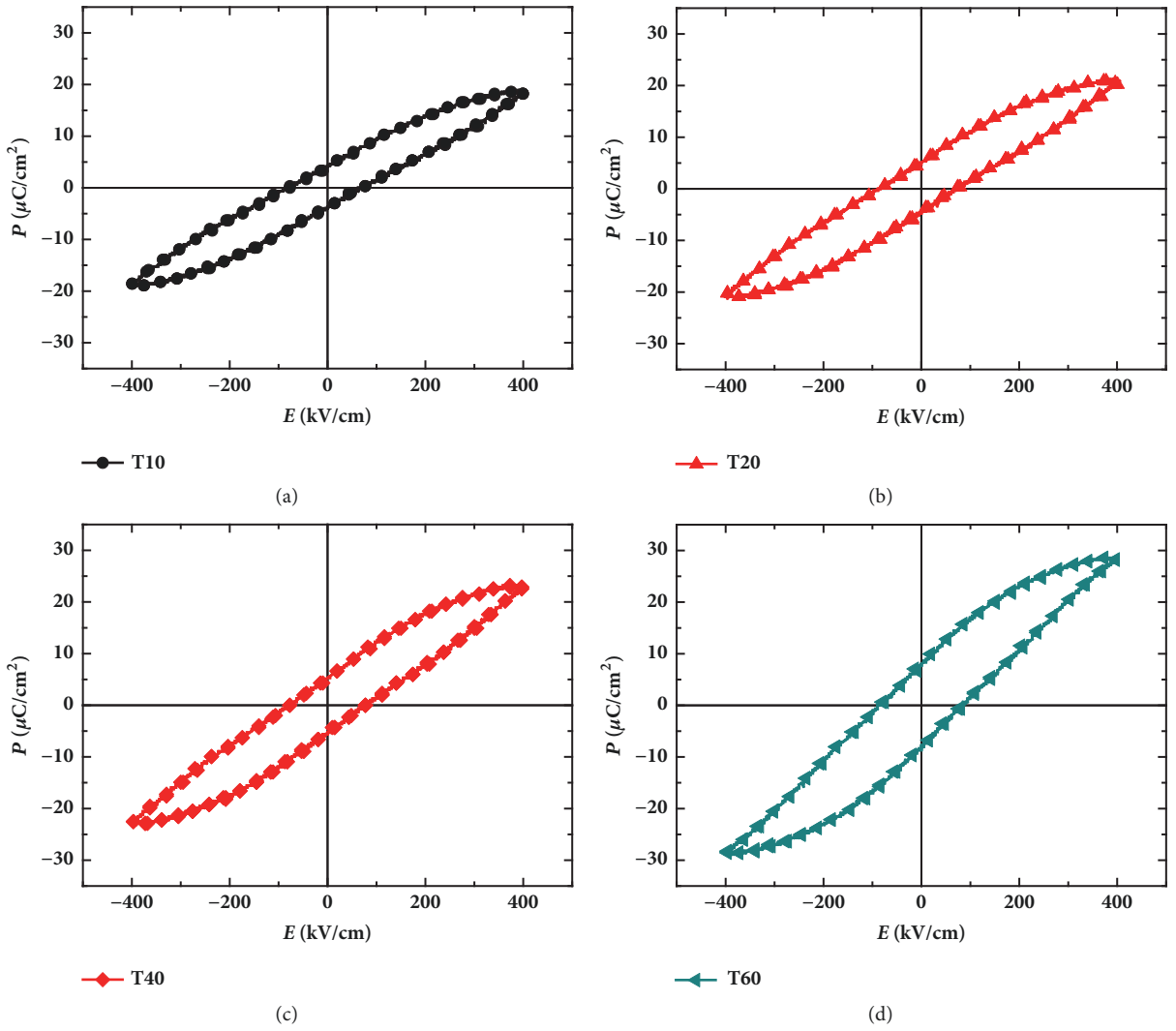

FIGURE 4: P–E ferroelectric hysteresis loops of BNKT films with different crystallization times at the same applied electric field of 400 kV/cm.

Based on (2) and (3), η value of the material can be calculated as follows:

$$\eta = \frac{J_{reco}}{J_{reco} + J_{loss}} \times 100 \quad (4)$$

Figure 5(b) demonstrates energy-storage density (J_{reco}), energy loss density (J_{loss}), and energy-storage efficiency (η) of the BNKT films as a function of crystallization time at applied electric field E_{appl} of 400 kV/cm. While J_{reco} and J_{loss} experience an increasing trend with a rise of crystallization time, the opposite is true of η. The BNKT films, annealed in 10 min, possess the small J_{reco} and J_{loss} values of 2.2 J/cm^3 and 1.2 J/cm^3, respectively. J_{reco} continuously increases from 2.2 J/cm^3 to 2.9 J/cm^3 as crystallization time rises from 10 min to 60 min. Similarly, J_{loss} reaches the highest value of about 2.0 J/cm^3. J_{reco} is obviously enhanced with an increase of annealing time. This matches up the improved polarization as analysed in Figure 4. But η follows a downward trend from 65.0% to 59.3%. This behaviour is related to an increase of the coercive electric field, caused by oxygen vacancies. When the BNKT films are annealed at high temperature, A-site metals (such as Bi^{3+}, Na^+, K^+) are evaporated, forming oxygen vacancies. With such J_{reco} and η values, the BNKT films are comparable with other lead-free films in terms of energy-storage ability and have potential application for electrostatic energy-storage devices.

4. Conclusions

Lead-free $Bi_{0.5}(Na_{0.80}K_{0.20})_{0.5}TiO_3$ ferroelectric films have been successfully fabricated on Pt/Ti/SiO_2/Si substrates via a spin coating assisted sol-gel method. The experimental results showed that all the films have well crystallized corresponding to the single-phase perovskite structure and no other impurity phases are detected. BNKT thin films obtained a significant enhancement in ferroelectric properties and energy-storage density by increasing the crystallization time. P_{m} and P_{r} of films reached their highest values of around 28.9 μC/cm^2 and 7.9 μC/cm^2, respectively, thanks to rising the crystallization time from 10 min to 60 min. Because

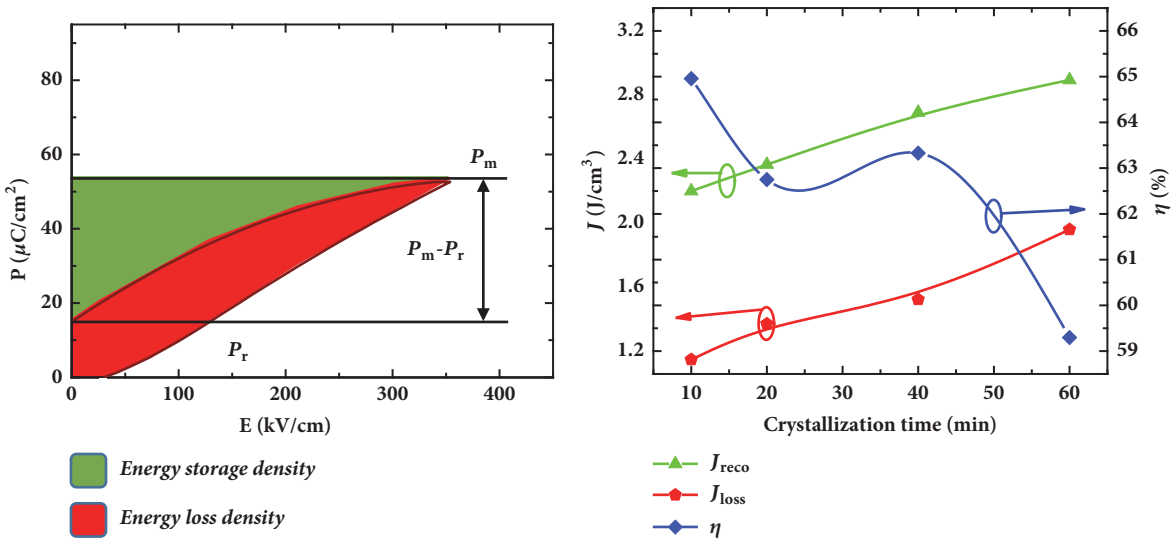

FIGURE 5: (a) Schematic diagram for the calculation of energy-storage properties of ferroelectric films, (b) energy-storage density (J_{reco}), energy loss density (J_{loss}), and energy-storage efficiency (η) of BNKT films at applied electric field E_{appl} of 400 kV/cm.

of large (P_m – P_r) polarization difference, J_{reco} got the maximum value of 2.9 J/cm^3. The obtained advantages are due to the intermediate pyrochlore phase which is completely transformed into the perovskite phase.

Data Availability

The data used to support the findings of this study are included within the article.

Conflicts of Interest

The authors declare that they have no conflicts of interest.

Acknowledgments

This research is funded by Vietnam National Foundation for Science and Technology Development (NAFOSTED) under grant number 103.02-2017.21.

References

[1] N. H. Fletcher, A. D. Hilton, and B. W. Ricketts, "Optimization of energy storage density in ceramic capacitors," *Journal of Physics D: Applied Physics*, vol. 29, no. 1, pp. 253–258, 1996.

[2] Y. Hao, X. Wang, K. Bi et al., "Significantly enhanced energy storage performance promoted by ultimate sized ferroelectric BaTiO3 fillers in nanocomposite films," *Nano Energy*, vol. 31, pp. 49–56, 2017.

[3] H. Pan, Y. Zeng, Y. Shen et al., "BiFeO3-SrTiO3 thin film as a new lead-free relaxor-ferroelectric capacitor with ultrahigh energy storage performance," *Journal of Materials Chemistry A*, vol. 5, no. 12, pp. 5920–5926, 2017.

[4] Y. Zhao, W. Yang, Y. Zhou et al., "Influence of molecular weight on the dielectric and energy storage properties of poly(vinylidene fluoride)," *Electronic Materials Letters*, vol. 12, no. 6, pp. 779–783, 2016.

[5] M. D. Nguyen, E. P. Houwman, M. Dekkers, C. T. Q. Nguyen, H. N. Vu, and G. Rijnders, "Research Update: Enhanced energy storage density and energy efficiency of epitaxial Pb0.9La0.1(Zr0.52Ti0.48)O3 relaxor-ferroelectric thin-films deposited on silicon by pulsed laser deposition," *APL Materials*, vol. 4, no. 8, 2016.

[6] I. Burn and D. M. Smyth, "Energy storage in ceramic dielectrics," *Journal of Materials Science*, vol. 7, no. 3, pp. 339–343, 1972.

[7] G. R. Love, "Energy Storage in Ceramic Dielectrics," *Journal of the American Ceramic Society*, vol. 73, no. 2, pp. 323–328, 1990.

[8] X. Hao, J. Zhai, and X. Yao, "Improved energy storage performance and fatigue endurance of Sr-Doped PbZrO3 antiferroelectric thin films," *Journal of the American Ceramic Society*, vol. 92, no. 5, pp. 1133–1135, 2009.

[9] M. Ye, Q. Sun, X. Chen, Z. Jiang, and F. Wang, "Effect of Eu doping on the electrical properties and energy storage performance of PbZrO 3 antiferroelectric thin films," *Journal of the American Ceramic Society*, vol. 94, no. 10, pp. 3234–3236, 2011.

[10] S. Tong, B. Ma, M. Narayanan et al., "Lead lanthanum zirconate titanate ceramic thin films for energy storage," *ACS Applied Materials & Interfaces*, vol. 5, no. 4, pp. 1474–1480, 2013.

[11] Z. Hu, B. Ma, S. Liu, M. Narayanan, and U. Balachandran, "Relaxor behavior and energy storage performance of ferroelectric PLZT thin films with different Zr/Ti ratios," *Ceramics International*, vol. 40, no. 1, pp. 557–562, 2014.

[12] B. Peng, Q. Zhang, X. Li et al., "Large Energy Storage Density and High Thermal Stability in a Highly Textured (111)-Oriented Pb0.8Ba0.2ZrO3 Relaxor Thin Film with the Coexistence of Antiferroelectric and Ferroelectric Phases," *ACS Applied Materials & Interfaces*, vol. 7, pp. 13512–13517, 2015.

[13] A. Chauhan, S. Patel, and R. Vaish, "Mechanical confinement for improved energy storage density in BNT-BT-KNN lead-free ceramic capacitors," *AIP Advances*, vol. 4, no. 8, 2014.

[14] P. Ge, X. Tang, Q. Liu, Y. Jiang, W. Li, and J. Luo, "Energy storage properties and electrocaloric effect of Ba0.65Sr0.35TiO3 ceramics near room temperature," *Journal of Materials Science: Materials in Electronics*, vol. 29, no. 2, pp. 1075–1081, 2017.

[15] Q. Xu, T. Li, H. Hao et al., "Enhanced energy storage properties of NaNbO3 modified Bi0.5Na0.5TiO3 based ceramics," *Journal of the European Ceramic Society*, vol. 35, no. 2, pp. 545–553, 2015.

[16] N. D. Quan, L. Huu Bac, D. V. Thiet, V. N. Hung, and D. D. Dung, "Current development in lead-free Bi0.5 (Na,K)0.5 TiO3 -based piezoelectric materials," *Advances in Materials Science and Engineering*, vol. 2014, pp. 1–13, 2014.

[17] G. Smolenskii, V. Isupov, A. Agranovskaya, and N. Krainik, "New ferroelectrics of complex composition," *Soviet Physics-Solid State*, vol. 2, pp. 2651–2654, 1961.

[18] L. Zhang, X. Hao, and L. Zhang, "Enhanced energy-storage performances of Bi2O3-Li 2O added (1-x)(Na0.5Bi0.5) TiO 3-xBaTiO3 thick films," *Ceramics International*, vol. 40, no. 6, pp. 8847–8851, 2014.

[19] Q. Xu, H. Liu, Z. Song et al., "A new energy-storage ceramic system based on Bi0.5Na0.5TiO3 ternary solid solution," *Journal of Materials Science: Materials in Electronics*, vol. 27, no. 1, pp. 322–329, 2016.

[20] X. Lu, J. Xu, L. Yang et al., "Energy storage properties of (Bi0.5Na0.5)0.93Ba0.07TiO3 lead-free ceramics modified by La and Zr co-doping," *Journal of Materiomics*, vol. 2, no. 1, pp. 87–93, 2016.

[21] W. P. Cao, W. L. Li, X. F. Dai et al., "Large electrocaloric response and high energy-storage properties over a broad temperature range in lead-free NBT-ST ceramics," *Journal of the European Ceramic Society*, vol. 36, no. 3, pp. 593–600, 2016.

[22] M. Yao, Y. Pu, H. Zheng, L. Zhang, M. Chen, and Y. Cui, "Improved energy storage density in 0.475BNT-0.525BCTZ with MgO addition," *Ceramics International*, vol. 42, no. 7, pp. 8974–8979, 2016.

[23] Y. Zhao, X. Hao, and M. Li, "Dielectric properties and energy-storage performance of (Na 0.5Bi0.5)TiO3 thick films," *Journal of Alloys and Compounds*, vol. 601, pp. 112–115, 2014.

[24] N. D. Quan, V. N. Hung, I. W. Kim, and D. D. Dung, "Bipolar electric field induced strain in li substituted lead-free bi0.5(na0.82k0.18)0.5ti0.95sn0.05o3 piezoelectric ceramics," *Journal of Nanoscience and Nanotechnology*, vol. 16, no. 8, pp. 7978–7982, 2016.

[25] N. D. Quan, T. Q. Toan, V. N. Hung, and M. Nguyen, "Influence of Crystallization Temperature on Structural, Ferroelectric, and Ferromagnetic Properties of Lead-Free $Bi_{0.5}(Na_{0.8}K_{0.2})_{0.5}TiO_3$ Multiferroic Films," *Advances in Materials Science and Engineering*, vol. 2019, Article ID 8976385, 8 pages, 2019.

[26] N. D. Quan, V. N. Hung, and D. D. Dung, "Influence of film thickness on ferroelectric properties and leakage current density in lead-free Bi0.5(Na0.80K0.20)0.5TiO3 films," *Materials Research Express*, vol. 4, no. 8, 2017.

[27] N. D. Quan, V. N. Hung, and D. D. Dung, "Effect of Zr Doping on Structural and Ferroelectric Properties of Lead-Free Bi0.5(Na0.80K0.20)0.5TiO3 Films," *Journal of Electronic Materials (JEM)*, vol. 46, no. 10, pp. 5814–5819, 2017.

[28] A. Monshi, M. R. Foroughi, and M. R. Monshi, "Modified scherrer equation to estimate more accurately nano-crystallite size using XRD," *World Journal of Nanoscience and Engineering*, vol. 2, no. 3, pp. 154–160, 2012.

[29] N. D. Quan, V. N. Hung, N. Van Quyet, H. V. Chung, and D. D. Dung, "Band gap modification and ferroelectric properties of Bi 0.5(Na,K)0.5TiO3-based by Li substitution," *AIP Advances*, vol. 4, no. 1, 2014.

[30] J. Anthoniappen, C. S. Tu, P.-Y. Chen, C.-S. Chen, Y. U. Idzerda, and S.-J. Chiu, "Raman spectra and structural stability in B-site manganese doped (Bi 0.5 Na 0.5) 0.925 Ba 0.075 TiO 3 relaxor ferroelectric ceramics," *Journal of the European Ceramic Society*, vol. 35, no. 13, pp. 3495–3506, 2015.

[31] P.-Y. Chen, C.-S. Chen, C.-S. Tu, P.-H. Chen, and J. Anthoniappen, "Effects of texture on microstructure, Raman vibration, and ferroelectric properties in 92.5%(Bi0.5Na0.5)TiO3–7.5%BaTiO3 ceramics," *Journal of the European Ceramic Society*, vol. 36, no. 7, pp. 1613–1622, 2015.

[32] N. D. Quan, N. V. Hong, T. Q. Toan, and V. N. Hung, "Enhanced ferroelectric properties and energy storage density in PLZT/BNKT heterolayered thin films prepared by sol-gel method," *The European Physical Journal B*, vol. 91, no. 12, p. 316, 2018.

[33] C. W. Ahn, S. S. Won, A. Ullah et al., "Large piezoresponse of lead-free Bi 0.5(Na 0.85K 0.15) 0.5TiO 3 thin film," *Current Applied Physics*, vol. 12, no. 3, pp. 903–907, 2012.

[34] H. Borkar, V. N. Singh, B. P. Singh, M. Tomar, V. Gupta, and A. Kumar, "Room temperature lead-free relaxor-antiferroelectric electroceramics for energy storage applications," *RSC Advances*, vol. 4, no. 44, pp. 22840–22847, 2014.